LARGE-STRAIN GENERALIZATION OF MICROPLANE MODEL FOR CONCRETE AND APPLICATION

By Zdeněk P. Bažant,[1] Fellow ASCE, Mark D. Adley,[2] Ignacio Carol,[3] Milan Jirásek,[4] Stephen A. Akers,[5] Bob Rohani,[6] J. Donald Cargile,[7] and Ferhun C. Caner[8]

ABSTRACT: The formulation of the microplane model for concrete and development of model M4 in the three preceding companion papers in this study is here extended to large strains. After giving examples of certain difficulties with the second Piola-Kirchhoff stress tensor in the modeling of strength and frictional limits on weak planes within the material, the back-rotated Cauchy (true) tensor is introduced as the stress measure. The strain tensor conjugate to the back-rotated Cauchy (or Kirchhoff) stress tensor is unsuitable because it is nonholonomic (i.e., path-dependent) and because its microplane components do not characterize meaningful deformation measures. Therefore Green's Lagrangian tensor is adopted, even though it is not conjugate. Only for this strain measure do the microplane components of the strain tensor suffice to characterize the normal stretch and shear angle on that microplane. Using such nonconjugate strain and stress tensors is admissible because, for concrete, the elastic parts of strains as well as the total volumetric strains are always small, and because the algorithm used guarantees the energy dissipation by large inelastic strains to be nonnegative. Examples of dynamic structural analysis are given.

INTRODUCTION

Under high hydrostatic pressures, quasibrittle materials such as concretes, rocks, and some composites can undergo very large strains exceeding 100% while retaining their integrity (Bažant et al. 1999). Such strains are, for instance, observed in measurements and numerical simulations of the impact of missiles into concrete walls and soil or rock masses, in blast and ground shock effects on hardened protective structures, in seismic response of highly confined concrete columns, and in longtime deformation of rock by geological processes. In the absence of high pressure, very large deformations can be exhibited by concrete that has been reduced to rubble and behaves like a soil.

An effective constitutive model for such problems is the microplane model. Its latest version for concrete, which was labeled M4 and was presented in the three other companion papers in this study (Bažant et al. 2000a,b; Caner and Bažant 2000), was confined to small strains. An approximate generalization of the microplane to large strains was given in Bažant et al. (1996), but was limited to moderately large strains (up to about 10%). The present study, which develops in detail the finite-strain formulation broadly outlined at a recent conference (Bažant 1997), will feature a generalization of the microplane model to arbitrarily large strains. In closing, examples of application in dynamic structural analysis will be given.

The problem will be approached with the stipulation that the large-strain model be obtainable by a simple generalization of an existing small-strain microplane model (such as model M4 presented in the other three parts of this study), without any refitting of the generalized model to the existing representative small-strain material test data. Because of this requirement, and because of the need to use microplane stress and strain measures that have a clear physical meaning, use is made of certain approximations justified for concrete by the smallness of the elastic parts of strains and of the inelastic volume changes. In this regard, it may be remarked that Carol et al. (1998) and Jirásek (1999) conceived rigorous thermodynamics-based finite-strain formulations of the microplane model that satisfy thermodynamic restrictions exactly, without any restrictions; however, they would require entire recalibration of the microplane model by material test data, which might prove hard because of certain practical difficulties (to be discussed later) in adopting conjugate stress and strain measures on the microplanes.

Since the microplane model has been described in the preceding three papers (Bažant et al. 2000a,b; Caner and Bažant 2000), a review of its basic concepts will not be necessary. All the definitions and notations will be retained.

MEASURES OF FINITE STRAIN AND STRESS

We will consider a broad class of finite strain measures called the Doyle-Ericksen tensors [Doyle and Ericksen (1956); see also Ogden (1984); Bažant and Cedolin (1991)]: for $m \neq 0$, $\boldsymbol{\varepsilon}^{(m)} = (\mathbf{U}^m - \mathbf{I})/m$; for $m = 0$, $\boldsymbol{\varepsilon}^{(m)} = \ln \mathbf{U}$, where m = parameter = any real number; $\mathbf{U} = \sqrt{\mathbf{C}}$; $\mathbf{C} = \mathbf{F}^T\mathbf{F}$ = Cauchy-Green deformation tensor (e.g., Ogden 1984; Bažant and Cedolin 1991). The right-stretch tensor, denoted as $\mathbf{U}$ is defined by the polar decomposition $\mathbf{F} = \mathbf{RU}$ of the deformation gradient $\mathbf{F} = \partial\mathbf{x}/\partial\mathbf{X}$, where $\mathbf{X}$ and $\mathbf{x}$ are the initial and final Cartesian coordinates of the material point (Malvern 1969; Ogden 1984; Bažant and Cedolin 1991). (The tensor products such as $\mathbf{RU}$ are singly contracted products; the dot symbol for product is omitted.)

The simplest to calculate is Green's Lagrangian strain tensor (e.g., Malvern 1969), proposed by Green and using Lagrangian coordinates:

$$\boldsymbol{\varepsilon} = \frac{1}{2}(\mathbf{F}^T\mathbf{F} - \mathbf{I}) \tag{1}$$

Green's Lagrangian tensor corresponds to $m = 2$. The case $m = 1$ yields the Biot strain tensor, and the case $m \to 0$ yields

[1]Walter P. Murphy Prof. of Civ. Engrg. and Mat. Sci., Northwestern Univ., Evanston IL 60208. E-mail: z_bazant@northwestern.edu
[2]Res. Engr., U.S. Army Engr. Waterways Experiment Station, Vicksburg, MI 31980-6199.
[3]Prof., Universidad Politecnica de Catalunya, Barcelona, Spain.
[4]Res. Engr., Swiss Federal Institute of Technology (EPFL), Lausanne, Switzerland.
[5]Res. Engr., U.S. Army Engr. Waterways Experiment Station, Vicksburg, MS.
[6]Res. Engr., U.S. Army Engr. Waterways Experiment Station, Vicksburg, MS.
[7]Res. Engr., U.S. Army Engr. Waterways Experiment Station, Vicksburg, MS.
[8]Grad. Res. Asst., Northwestern Univ., Evanston, IL.

Note. Associate Editor: Gilles Pijaudier-Cabot. Discussion open until February 1, 2001. Separate discussions should be submitted for the individual papers in this symposium. To extend the closing date one month, a written request must be filed with the ASCE Manager of Journals. The manuscript for this paper was submitted for review and possible publication on March 2, 1999. This paper is part of the ***Journal of Engineering Mechanics***, Vol. 126, No. 9, September, 2000. ©ASCE, ISSN 0733-9399/00/0009-0971–980/$8.00 + $.50 per page. Paper No. 20386.

the Hencky (logarithmic) strain tensor (Hencky 1928; Ogden 1984; Bažant and Cedolin 1991; Rice 1993). The stress tensor **S**, called conjugate, for which $\mathbf{S}:d\boldsymbol{\varepsilon}$ (where : stands for a doubly contracted product) is the correct work expression, is the second Piola-Kirchhoff stress tensor. It is related to the Cauchy (true) stress tensor σ as follows:

$$\mathbf{S} = \mathbf{F}^{-1}J\boldsymbol{\sigma}\mathbf{F}^{-T} \quad \text{or} \quad \boldsymbol{\sigma} = J^{-1}\mathbf{F}\mathbf{S}\mathbf{F}^{T} \tag{2}$$

with the notation $\mathbf{F}^{-T} = (\mathbf{F}^{-1})^T = (\mathbf{F}^T)^{-1}$ (Malvern 1969; Ogden 1984; Bažant and Cedolin 1991).

Two simple examples of an elastic constitutive equation for isotropic materials in finite strain may be written as

$$1\text{: } \tilde{S}_{ij} = \Lambda\tilde{\varepsilon}_{kk}\delta_{ij} + 2G\tilde{\varepsilon}_{ij} \tag{3}$$

$$2\text{: } \tilde{S}_{ij} = 3K\tilde{\varepsilon}_V\delta_{ij} + 2G\tilde{\varepsilon}_{Dij} \tag{4}$$

Here δ_{ij} = Kronecker delta (unit tensor components); $\tilde{\varepsilon}_{ij}$ = components of finite strain tensor $\tilde{\boldsymbol{\varepsilon}}$ of any type of Cartesian coordinates x_i (i = 1, 2, 3); $\tilde{S}_{ij}$ = components of stress tensor **S** that is conjugate to $\tilde{\boldsymbol{\varepsilon}}$; repetition of coordinate subscripts implies summation over i = 1, 2, 3; and Λ, G = elastic constants analogous to Lamé elastic constant (note that $K = \Lambda + 2G/3$ = constant that is formally analogous to the bulk modulus but does not have such physical meaning because, for large strains, the trace $\tilde{\varepsilon}_{kk}$ is not the volume change). Furthermore, $\tilde{\varepsilon}_V = \varepsilon_0 + \varepsilon_0^2/2$ = volumetric strain = Green's Lagrangian normal strain component corresponding to the isotropic (volumetric) stretch that gives the exact relative volume change; $\varepsilon_0 = (J - 1)/3$ = linearized (small) volumetric strain; J = det **F** = Jacobian of the transformation; and $\tilde{\varepsilon}_{Dij} = \tilde{\varepsilon}_{ij} - \tilde{\varepsilon}_V\delta_{ij}$ = components of the deviatoric strain tensor $\tilde{\boldsymbol{\varepsilon}}_D$ defining an isochoric deformation (i.e., deformation at constant volume) according to the additive decomposition proposed by Bažant (1996).

The decomposition of the displacement gradient tensor (transformation tensor) of large deformation into its volumetric and deviatoric (strictly speaking, isochoric) parts is in general, multiplicative. It has the form $\mathbf{U} = \mathbf{F}_D\mathbf{U}_V$ (Flory 1961; Sidoroff 1974; Bell 1985; Simo and Ortiz 1985; Lubliner 1986; Simo 1988) where **U** = right stretch tensor; $\mathbf{U}_V$ = volumetric right-stretch tensor; and $\mathbf{F}_D$ = deviatoric transformation tensor.

For concrete, as well as many other materials, the volumetric-deviatoric decomposition is simplified by the fact that the volumetric strain ε_V is always small (it is about -3% at the highest pressure tested so far, which was 300,000 psi or 2,069 MPa; Bažant et al. 1986). This is small enough to permit writing the volumetric-deviatoric split of Green's Lagrangian strain approximately as additive (Bažant 1996). In component form, $\varepsilon_{ij} = \varepsilon_{Dij} + \varepsilon_V\delta_{ij}$, where ε_V = exact volumetric strain for the given strain measure. For Green's Lagrangian strain measure, $\varepsilon_V = \varepsilon_0 + \varepsilon_0^2/2$. For the Biot strain measure (Biot 1965; Ogden 1984; Bažant and Cedolin 1991), $\varepsilon_V = J^{1/3} - 1$, in which case the volume change magnitude could be up to about 8% to permit additive decomposition. The additive decomposition is exact if and only if the strain measure is the Hencky (logarithmic) strain tensor **H**, in which case $\varepsilon_V = (\ln J)/3$.

Thus the classical multiplicative decomposition, which is less convenient for calculations than the additive decomposition, appears to be inevitable only for materials exhibiting very large volume changes, such as stiff foams.

DIFFICULTIES WITH PHYSICAL MEANING OF CONJUGATE STRESS TENSOR

What makes the microplane model conceptually simple, and more realistic than the classical (macroscopic) constitutive equations expressed in terms of tensors and their invariants, is that the normal and shear stress components on the microplanes are directly used to describe physical phenomena such as friction and strength or yield limit. This approach, however, makes sense only if the stress components on the microplanes characterize the true stresses on planes of various orientations within the material. Let us now examine whether this is the case for the second Piola-Kirchhoff stress tensor **S**.

While for elastic deformations only certain combinations of **S** and $\boldsymbol{\varepsilon}$ can arise, for inelastic deformations almost any combination can. As a special case, we consider in this section that the material rotation is zero ($\mathbf{R} = \mathbf{I}$), that the stress and strain tensors are coaxial, and that Cartesian coordinates x_i are placed in the principal stress directions, as follows:

$$\mathbf{F} = \mathbf{U} = \begin{bmatrix} \lambda_1, & 0, & 0 \\ 0, & \lambda_2, & 0 \\ 0, & 0, & \lambda_3 \end{bmatrix}; \quad \boldsymbol{\sigma} = \begin{bmatrix} \sigma_1, & 0, & 0 \\ 0, & \sigma_2, & 0 \\ 0, & 0, & \sigma_3 \end{bmatrix} \tag{5a,b}$$

where λ_1, λ_2, λ_3 = principal stretches and σ_1, σ_2, σ_3 = principal Cauchy stresses. Then

$$\mathbf{S} = \begin{bmatrix} \sigma_1\lambda_2\lambda_3/\lambda_1, & 0, & 0 \\ 0, & \sigma_2\lambda_3\lambda_1/\lambda_2, & 0 \\ 0, & 0, & \sigma_3\lambda_1\lambda_2/\lambda_3 \end{bmatrix} \tag{6}$$

The shear component of **S** on the plane forming angles 45° with coordinate planes (x_1, x_3) and (x_2, x_3) is $S'_{12} = (S_1 - S_2)/2 = [\sigma_1(\lambda_2\lambda_3/\lambda_1) - \sigma_2(\lambda_3\lambda_1/\lambda_2)]/2$, while the corresponding Cauchy stress component is $\sigma'_{12} = (\sigma_1 - \sigma_2)/2$. The normal component of **S** on the octahedral plane is $S_{\text{oct}} = [\sigma_1(\lambda_2\lambda_3/\lambda_1) + \sigma_2(\lambda_3\lambda_1/\lambda_2) + \sigma_3(\lambda_1\lambda_2/\lambda_3)]/3$, while the normal component of Cauchy stress on that plane is the mean Cauchy stress $\sigma_{\text{oct}} = (\sigma_1 + \sigma_2 + \sigma_3)/3 = -p$ (p = hydrostatic pressure). Another similar difference could be demonstrated for the magnitudes of shear stresses on the octahedral plane, which are given by $\sqrt{2J_2(\mathbf{S})/3}$ and $\sqrt{2J_2(\boldsymbol{\sigma})/3}$, where J_2 denotes the second deviator invariant of the tensor.

Obviously, for large stretches such as 2 or 1/2, the components of the second Piola-Kirchhoff stress tensor can differ enormously from the corresponding components of the Cauchy stress tensor (for the deformations of finite elements in missile impact simulations, easily by a factor of 2 or more). Consequently, the limit condition of frictional slip on a certain plane cannot be formulated in terms of **S** alone, and neither can the limit conditions of yield or strength limit, or the law of strain hardening or strain softening on that plane. Frictional slip on a certain plane, for example, depends on the true normal and shear stresses on a section by that plane through the deformed material, and not directly on the stresses transformed to a section of the material in its virgin initial state.

Although large elastic deformations are not the concern of this study, the difficulties with the physical interpretation of constitutive relations can be instructively manifested by considering the elastic stress produced by biaxial isochoric deformations without rotation ($\mathbf{R} = \mathbf{I}$) defined by principal stretches $\lambda_1 = \lambda$, $\lambda_2 = 1/\lambda$, $\lambda_3 = 1$, for which the principal Green's Lagrangian strains are $\varepsilon_1 = (\lambda^2 - 1)/2$, $\varepsilon_2 = (\lambda^{-2} - 1)/2$, and $\varepsilon_3 = 0$ (and $J = 1$). Adopting, for instance, the simple stress-strain relation (4), we have $\varepsilon_V = 0$, $\varepsilon_{Dij} = \varepsilon_{ij}$ and $S_{ij} = 2G\varepsilon_{ij}$. For the mean stress value of the second Piola-Kirchhoff tensor, we get $S_{kk}/3 = (\lambda - \lambda^{-1})^2G/3 \geq 0$. Using (2), we obtain for the Cauchy stress tensor the mean stress value $\sigma_{kk}/3 = (\lambda^4 - \lambda^2 - \lambda^{-2} + \lambda^{-4})G/3 = (\lambda^6 - 1)(\lambda^2 - 1)\lambda^{-4}G/3 \geq 0$. For $\lambda = 1.1$ and 2, (4) yields $S_{kk}/3 = 0.01215G$ and $0.75G$, respectively, and $\sigma_{kk}/3 = 0.03689G$ and $3.896G$. If, instead of (4), we use the stress-strain relation (3), we get the same result, except that the foregoing mean stress value must be multiplied by the ratio $1 + (3\lambda/2G)$. These values of the mean true stress caused by elastic isochoric deformation are not only nonzero, but enormous. Even though we do not need to worry about large elastic strains of materials such as concrete, this example blatantly demonstrates that a constitutive law in terms of the sec-

ond Piola-Kirchhoff stress does not allow a simple control of hydrostatic pressure, and thus also of pressure sensitivity, internal friction, and dilatancy of material.

The physical meaning of the microplane stress components must be clear enough to allow on a particular plane of normal **n** simple modeling of (1) friction; (2) yield limit; and (3) strain softening. As an example, consider that coordinates (x_1', x_2') form angle $\pi/4$ with (x_1, x_2) and $x_3' \equiv x_3$. The true friction ratio on the plane normal to x_1' in terms of the true (Cauchy) stresses and the second Piola-Kirchhoff stresses are found to be $k = \sigma_{12}'/\sigma_{11}' = (\sigma_1 - \sigma_2)/(\sigma_1 + \sigma_2)$ and $k = S_{12}'/S_{11}' = (\sigma_1\lambda_2^2 - \sigma_1\lambda_1^2)/(\sigma_1\lambda_2^2 + \sigma_1\lambda_1^2)$. Consider, for example, that $\lambda_3 = 1$, $\lambda_1 = 1/2$, and $\lambda_2 = 2$. Then, for $\sigma_1 = \sigma_2$, we get $k = 0$ and $\bar{k} = 15/17$; for $\sigma_1 = 2\sigma_2$, we get $k = 1/3$ and $\bar{k} = 31/35$; and for $\sigma_2 = -\sigma_1$, we get $k = \infty$ and $\bar{k} = -17/15$.

Further, let σ_0 denote the yield limit for normal stress σ_N or S_N. On the plane normal to x_1', we then have the yield conditions $\sigma_N = \sigma_{11}' = (\sigma_1 + \sigma_2)/2$ and $S_N = S_{11}' = (\sigma_1\lambda_2/\lambda_1 + \sigma_2\lambda_1/\lambda_2)/2$. Consider again that $\lambda_3 = 1$, $\lambda_1 = 1/2$, and $\lambda_2 = 2$. Then for $\sigma_1 = \sigma_2$, these yield conditions are $\sigma_N = \sigma_1 = \sigma_0$ and $S_N = (17/8)\sigma_1 = \sigma_0$, and for $\sigma_1 > 0$ and $\sigma_2 = 0$, they are $\sigma_N = 1/2 = \sigma_0$ and $S_N = (1/8)\sigma_1 = \sigma_0$.

Finally, consider strain softening characterized in terms of Cauchy stress by $\sigma_N = (\lambda_N - 1)E_N/\omega$, where ω = damage variable. Conversely, $\omega = 1 - (\lambda_N - 1)E_N/\sigma_N$. If σ_N is replaced by the second Piola-Kirchhoff stress S_N, $\bar{\omega} = 1 - (\lambda_N - 1)E_N/S_N$. The stretch $\lambda_{11}' = \lambda_N$ in the x_1' direction is calculated as follows:

$$\vec{\lambda}_N = \mathbf{n}\cdot\mathbf{F} = (\lambda_1/\sqrt{2},\ \lambda_2/\sqrt{2}); \quad \lambda_N = \sqrt{\frac{1}{2}(\lambda_1^2 + \lambda_2^2)} \qquad (7a,b)$$

If we consider $\sigma_1 = \sigma_2$, $\lambda_2 = \lambda_1 = \lambda_{11}' = \lambda_N = 2$, we get for damage in terms of Cauchy stress $\omega = 1 - E_N/\sigma_1$, and for damage in terms of second Piola-Kirchhoff stress $\bar{\omega}_N = 1 - 2(\lambda_N - 1)E_N/(\lambda_1^{-2} + \lambda_1^2)\sigma_1 = 1 - 8E_N/17\sigma_1$. When $\omega = 1/2$, $\bar{\omega} = 13/17$.

In the foregoing examples, replacement of Cauchy stress with the second Piola-Kirchhoff stress is seen to produce enormous differences. The Cauchy stress, representing the true stress, must be considered as the correct one. Similar difficulties can be demonstrated for Biot's stress.

CHOICE OF STRESS TENSOR FOR MICROPLANE MODEL

The problem of formulating the large-strain constitutive relation of the microplane model for concrete is not the same as for elastomers such as rubber. For the latter, the problem is easier because the material is elastic, which means that the potential energy can be assumed to be a simple function (e.g., a low degree polynomial) of the invariants of the finite-strain tensor. Any finite strain tensor can be used, and no physical concepts such as the internal friction, yield limit, and pressure sensitivity are needed in that case; but for inelastic materials, the situation is very different.

In view of the foregoing examples, it is not surprising that the previous attempts to develop a reasonably performing large-strain microplane model in terms of the second Piola-Kirchhoff stress tensor have met with no success. The same is true of the stress tensor conjugate to the Biot strain tensor.

The Cauchy (true) stress tensor would give a clear physical meaning for the microplane stress components, but since this tensor is not referred to the initial configuration of the material and is not conjugate to any Lagrangian finite strain tensor, it cannot be used in a constitutive equation for a material such as concrete that has a memory of the initial state. This stress tensor is conjugate to the deformation rate (or velocity strain).

What is then the proper stress tensor to use? It is the Cauchy (true) stress tensor rotated back to the initial coordinates **X** attached to the material:

$$\mathbf{s} = \mathbf{R}^T\boldsymbol{\sigma}\mathbf{R} \qquad (8)$$

where $\boldsymbol{\sigma}$ = Cauchy stress (true stress) tensor; and **R** = material rotation tensor. In the case of no rotation, **s** coincides with the Cauchy stress tensor.

Another possible choice could be the back-rotated Kirchhoff stress tensor, which is obtained by scaling **s** with the scalar J, that is, $\boldsymbol{\tau} = \mathbf{R}^T J\boldsymbol{\sigma}\mathbf{R}$, where $J\boldsymbol{\sigma}$ = Kirchhoff stress tensor. The true stresses are easily figured out by dividing the components of the back-rotated Kirchhoff stress tensor by scalar J. This tensor has been used by Hoger (1987), Eterovic and Bathe (1990), and Gabriel and Bathe (1995) for incremental description of plastic materials in large strain.

The back-rotated Cauchy or Kirchhoff stress tensor has the property that $\mathbf{s} = \boldsymbol{\sigma}$ (=Cauchy stress tensor) or $\boldsymbol{\tau} = \boldsymbol{\sigma}/J$, respectively, if there is no coordinate rotation ($\mathbf{R} = \mathbf{I}$). If there is nonzero rotation **R**, the physical meaning of stresses does not get changed by the rotation; only the component values get transformed. The hydrostatic pressure, which is important for pressure-sensitive materials such as concrete, soils, or rocks, is given by tr **s** or (tr **s**)/3J, respectively. This is true regardless of rotation **R** because the trace of a tensor is an invariant. The second invariant of the deviator of **s** is equal, regardless of rotation, to the second invariant of tensor $\boldsymbol{\sigma}$ because any invariant is, by definition, unaffected by rotation.

A constitutive law in terms of the back-rotated Cauchy stress or back-rotated Kirchhoff stress could, in principle, be always transformed to a constitutive relation in terms of the second Piola-Kirchhoff stress. But then the constitutive law would no longer be expressed in terms of stress and strains on a single microplane alone.

CHOICE OF FINITE STRAIN TENSOR FOR MICROPLANE MODEL

It would seem appropriate to choose as the strain measure the strain tensor that is work-conjugate to the chosen stress tensor. However, two distinct problems would arise.

The first problem is that the strain tensor conjugate to the back-rotated Cauchy stress tensor, as well as that conjugate to the back-rotated Kirchhoff stress tensor, is nonholonomic. In other words, it depends not only on the current deformation gradient, but also on the deformation path in which the current state has been reached. It may be shown (Appendix I) that the strain tensors **e** and $\boldsymbol{\xi}$ conjugate to **s** and $J\boldsymbol{\sigma}$, respectively, are defined incrementally by $d\mathbf{e} = J(\mathbf{U}^{-1}d\mathbf{U} + d\mathbf{U}\mathbf{U}^{-1})/2 = J\,\mathrm{sym}(\mathbf{U}^{-1}d\mathbf{U})$ and $d\boldsymbol{\xi} = (\mathbf{U}^{-1}d\mathbf{U} + d\mathbf{U}\mathbf{U}^{-1})/2 = \mathrm{sym}(\mathbf{U}^{-1}d\mathbf{U})$. If the principal strain axes do not rotate, integration yields the following expressions, of which the first one, representing the Hencky (logarithmic) strain tensor, is explicitly integrable and thus path-independent:

$$\boldsymbol{\xi} = \int \begin{bmatrix} d\lambda_1/\lambda_1, & 0, & 0 \\ 0, & d\lambda_2/\lambda_2, & 0 \\ 0, & 0, & d\lambda_3/\lambda_3 \end{bmatrix} = \begin{bmatrix} \ln\lambda_1, & 0, & 0 \\ 0, & \ln\lambda_2, & 0 \\ 0, & 0, & \ln\lambda_3 \end{bmatrix} \qquad (9)$$

$$\mathbf{e} = \int \begin{bmatrix} \lambda_2\lambda_3 d\lambda_1, & 0, & 0 \\ 0, & \lambda_3\lambda_1 d\lambda_2, & 0 \\ 0, & 0, & \lambda_1\lambda_2\lambda_3 \end{bmatrix} \qquad (10)$$

A nonholonomic (path-dependent) strain tensor evaluated incrementally has recently been adopted by Levitas (1996) for plastic metals. However, such a strain tensor appears questionable for materials for which the initial virgin state is an important reference for defining the constitutive behavior, such as the fracturing damage in concrete. The path-dependence destroys memory of the initial virgin state of a material.

The second problem lies in physical interpretation of the strain tensor components on various planes. To generalize the microplane model to finite strain, a definite physical meaning needs to be attached to the normal and shear strain components on the microplanes. The following two conditions ought to be met:

- *Condition I.* The normal strain component e_N on a microplane should uniquely characterize the stretch λ_N of a material line segment whose direction **n** is initially normal to the microplane. The component e_N should be independent of the stretches of the material line segments in other initial directions.
- *Condition II.* The shear strain components θ_{NL} (or θ_{LN}) should uniquely characterize the change of angle θ_{NM} or θ_{NL} between two initially orthogonal line segments of material points initially coinciding with unit vectors **n** and **m**, or **n** and **l**. These components should be independent of the stretch in any direction and of the angle change in planes other than (**n**, **m**) or (**n**, **l**).

As an example, consider a plane in the material (or a microplane) whose unit normal **n** has the components $\mathbf{n} = (n_1, n_2, n_3) = (1/\sqrt{2}, 1/\sqrt{2}, 0)$. First consider the normal strain. For any type of finite strain tensor $\tilde{\boldsymbol{\varepsilon}}$, $\tilde{\varepsilon}_N = n_i n_j \tilde{\varepsilon}_{ij} = n_1^2\tilde{\varepsilon}_1 + n_2^2\tilde{\varepsilon}_2 + n_3^2\tilde{\varepsilon}_3 = (\tilde{\varepsilon}_1 + \tilde{\varepsilon}_2)/2$. The normal strain component on the microplane is, for Green's Lagrangian strain, $\varepsilon_N = n_i n_j \varepsilon_{ij} = (\varepsilon_1 + \varepsilon_2)/2 = (\lambda_1^2 + \lambda_2^2 - 2)/4$; for the Biot strain, $e_N = n_i n_j e_{ij} = (e_1 + e_2)/2 = (\lambda_1 + \lambda_2)/2 - 1$; and for the Hencky strain, $H_N = n_i n_j H_{ij} = (H_1 + H_2)/2 = (\ln \lambda_1 + \ln \lambda_2)/2 = \ln \sqrt{\lambda_1\lambda_2}$. The stretch λ_N in the direction normal to the microplane is related to Green's Lagrangian strain as follows:

$$\varepsilon_N = \frac{1}{2}(\lambda_N^2 - 1) = f(\lambda_N) \tag{11}$$

[e.g., Malvern (1969), p. 164]. Denoting $\rho = \lambda_2/\lambda_1$ = ratio of principal stretches, we have $\lambda_1 = \lambda_N\sqrt{2/(1 + \rho^2)}$. Upon substitution into the foregoing equations, we obtain the following expressions for the Biot strain and Hencky strain:

$$e_N = \frac{1}{2}(1 + \rho)\lambda_1 - 1 = \lambda_N(1 + \rho)/(\sqrt{2(1 + \rho^2)}) - 1 = g(\lambda_N, \rho) \tag{12}$$

$$H_N = \ln(\lambda_1\sqrt{\rho}) = \ln(\lambda_N\sqrt{2\rho/(1 + \rho^2)}) = h(\lambda_N, \rho) \tag{13}$$

Now we notice that the expressions (12) and (13) for the Biot and Hencky normal strain components depend not only on the stretch λ_N in the direction normal to the microplane, but also on the ratio ρ of the stretches along the axes x_1, x_2. Thus they violate the aforementioned condition I.

But is this violation significant? It is. This is seen by evaluating (12) and (13) for the following cases, in all of which $\varepsilon_N = (\lambda_N^2 - 1)/2$:

$$\text{for } \rho = 1\text{: } e_N = \lambda_N - 1; \quad H_N = \ln \lambda_N \tag{14}$$

$$\text{for } \rho = \frac{10}{11} \text{ or } \frac{11}{10}\text{: } e_N = 0.9989\lambda_N - 1; \quad H_N = \ln(0.9977\lambda_N) \tag{15}$$

$$\text{for } \rho = \frac{3}{4} \text{ or } \frac{4}{3}\text{: } e_N = 0.9899\lambda_N - 1; \quad H_N = \ln(0.9798\lambda_N) \tag{16}$$

$$\text{for } \rho = \frac{1}{2} \text{ or } 2\text{: } e_N = 0.9487\lambda_N - 1; \quad H_N = \ln(0.8907\lambda_N) \tag{17}$$

$$\text{for } \rho = \frac{1}{4} \text{ or } 4\text{: } e_N = 0.8575\lambda_N - 1; \quad H_N = \ln(0.6860\lambda_N) \tag{18}$$

So we must conclude that for normal stretches λ_N between 0.78 and 1.30, the error in the normal microplane strain caused by ignoring the stretches in other orientations is about 1% of that strain for the case of the Biot strain measure and 2% for the case of the Hencky strain measure. Calculating other examples, one finds that this magnitude of error is just about the worst possible. So, in this range of moderately large strains (considered in Bažant et al. 1996), finite strain measures of all the common types ($|m| \leq 2$) are admissible for the microplane.

However, for normal stretches λ_N varying between 0.25 and 4 (or 0.5 and 2), the variation caused by stretches in other orientations is about 14% (or 5%) of the normal strain for the Biot strain measure, and 31% (or 11%) of the normal strain for the Hencky strain measure. The latter value also applies to the nonholonomic strain tensor conjugate to the back-rotated Kirchhoff stress, and a similar value applies to the nonholonomic strain tensors associated with the back-rotated Cauchy stress. Such variation is unacceptable. Therefore, no strain measure other than Green's Lagrangian strain tensor is suitable for the microplane model at very large strains. Such strains arise, for example, in finite-element analysis of missile penetration through concrete walls.

It must be emphasized that this is strictly a requirement of simplicity in the formulation of the microplane constitutive equation. Of course, one type of strain tensor can always be transformed to another and its components on the microplanes evaluated. But for other than Green's Lagrangian strain measures, the formulation of the large-strain constitutive law for one microplane ceases to be independent of the other microplanes, which would enormously complicate constitutive modeling.

Second, consider the microplane shear strains λ_{NM} and λ_{NL} (with the subscripts referring to orthogonal axes **n**, **m**, and **l**). They should uniquely characterize the previously defined shear angles θ_{NL} and θ_{NM} (thereby satisfying the aforementioned condition II). These angles may be calculated from the microplane components of Green's Lagrangian strain tensor:

$$\theta_{NL} = \arctan\left(\frac{(1 + 2\varepsilon_N)(1 + 2\varepsilon_L)}{4\varepsilon_L^2} - 1\right)^{-1/2} \tag{19}$$

the expression for θ_{NM} being similar [e.g., Malvern (1969), p. 166]. For large strains, the microplane shear stresses should in principle be calculated from these shear angles instead of the shear components of Green's Lagrangian strain tensor. However, in the finite strain generalization of model M4, these expressions are not needed.

In the case of Biot or Hencky finite strain measures, or any strain measure other than Green's Lagrangian, the finite shear angles on a microplane cannot be expressed solely in terms of the strain components on that microplane. They also depend on the shear angles on other planes and on the stretches in other directions, which violates condition II. These violations are tolerable only for moderately large principal stretches, roughly within the same range as mentioned before. Again, the conclusion is that Green's Lagrangian strain tensor is the strain measure to use in the microplane model for very large strains. Only for that tensor do the components on some plane suffice to define the geometry of deformation on that plane.

The fact that conditions I and II are satisfied only by Green's Lagrangian tensor does not come as a surprise if we realize that the metric of space is quadratic, and this tensor is the only quadratic tensor. The equilibrium conditions, by contrast, are linear. This portends problems with conjugacy of the stress tensor, which we discuss next.

USE OF NONCONJUGATE STRESS-STRAIN PAIRS

Based on the preceding analysis, the microplane model needs to employ Green's Lagrangian strain tensor coupled with either the back-rotated Cauchy stress or the back-rotated Kirchhoff stress. Of these two, the former is somewhat more convenient. Obviously, we thus have a nonconjugate stress strain pair. Is that admissible? In this regard, we need to examine several problems.

Unique Correspondence to Conjugate Constitutive Law

We want to use the nonconjugate constitutive law: $\boldsymbol{\tau} = \boldsymbol{\psi}(\boldsymbol{\varepsilon})$, where $\boldsymbol{\psi}$ = a tensorial function. We seek the relation to the conjugate constitutive law $\mathbf{S} = \boldsymbol{\phi}(\boldsymbol{\varepsilon})$, where $\boldsymbol{\phi}$ = tensorial function. To this end, we substitute this into (2), that is, into $\boldsymbol{\sigma} = J^{-1}\mathbf{F}\mathbf{S}\mathbf{F}^T$, in which we further substitute $\mathbf{F} = \mathbf{R}\mathbf{U}$ and $\mathbf{U} = \sqrt{\mathbf{I} + 2\boldsymbol{\varepsilon}} = \mathbf{U}(\boldsymbol{\varepsilon})$. This furnishes $\boldsymbol{\sigma} = J^{-1}\mathbf{R}\mathbf{U}(\boldsymbol{\varepsilon})\boldsymbol{\phi}(\boldsymbol{\varepsilon})\mathbf{U}(\boldsymbol{\varepsilon})\mathbf{R}^T$. Multiplying by $\mathbf{R}^T$ from the left and by $\mathbf{R}$ from the right, and substituting $\mathbf{R}^T\boldsymbol{\sigma}\mathbf{R} = \mathbf{s}$, we thus obtain

$$\mathbf{s} = \boldsymbol{\psi}(\boldsymbol{\varepsilon}); \quad \boldsymbol{\psi}(\boldsymbol{\varepsilon}) = \mathbf{U}(\boldsymbol{\varepsilon})\boldsymbol{\phi}(\boldsymbol{\varepsilon})\mathbf{U}(\boldsymbol{\varepsilon}) \qquad (20a,b)$$

$$\boldsymbol{\phi}(\boldsymbol{\varepsilon}) = \mathbf{U}^{-1}(\boldsymbol{\varepsilon})J\boldsymbol{\psi}(\boldsymbol{\varepsilon})\mathbf{U}^{-1}(\boldsymbol{\varepsilon}) \qquad (20c)$$

Admissibility of the nonconjugate constitutive law $\mathbf{s} = \boldsymbol{\psi}(\boldsymbol{\varepsilon})$ requires that the tensorial function $\boldsymbol{\psi}(\boldsymbol{\varepsilon})$ defining this law be uniquely related to function $\boldsymbol{\phi}(\boldsymbol{\varepsilon})$ and that this relation not involve material rotation $\mathbf{R}$. Obviously these conditions are satisfied. The same can be proven for a constitutive law using the back-rotated Kirchhoff stress tensor $\boldsymbol{\tau}$.

Generally, any finite strain tensor $\tilde{\boldsymbol{\varepsilon}}$ (referred to the initial configuration) can be combined in the constitutive law with the back-rotated Kirchhoff stress tensor $\boldsymbol{\tau}$. Stress $\tilde{\mathbf{S}}$ that is conjugate to an arbitrary finite strain tensor $\tilde{\boldsymbol{\varepsilon}}$ is defined by the variational work relation $\tilde{\mathbf{S}}{:}\delta\tilde{\boldsymbol{\varepsilon}} = \mathbf{S}{:}\delta\boldsymbol{\varepsilon}$, which may be written as $\tilde{\mathbf{S}}{:}[\boldsymbol{\Phi}(\tilde{\boldsymbol{\varepsilon}}){:}\delta\boldsymbol{\varepsilon}] = \mathbf{S}{:}\delta\boldsymbol{\varepsilon}$, where $\boldsymbol{\Phi}(\tilde{\boldsymbol{\varepsilon}}) = \partial\tilde{\boldsymbol{\varepsilon}}/\partial\boldsymbol{\varepsilon}$. Function $\boldsymbol{\Phi}$ is a fourth-order tensor. Consequently (Bažant 1996)

$$\mathbf{S} = \tilde{\mathbf{S}}{:}\boldsymbol{\Phi}(\tilde{\boldsymbol{\varepsilon}}); \quad \boldsymbol{\Phi}(\tilde{\boldsymbol{\varepsilon}}) = \partial\tilde{\boldsymbol{\varepsilon}}/\partial\boldsymbol{\varepsilon} \qquad (21a,b)$$

Now let us carry out the following transformations:

$$\mathbf{s} = \mathbf{R}^T\boldsymbol{\sigma}\mathbf{R} = \mathbf{R}^T(\mathbf{F}\mathbf{S}\mathbf{F}^T)\mathbf{R}J^{-1} = \mathbf{U}\mathbf{S}\mathbf{U}J^{-1}$$

$$= \mathbf{U}[\tilde{\mathbf{S}}{:}\boldsymbol{\Phi}(\tilde{\boldsymbol{\varepsilon}})]\mathbf{U}J^{-1} = \mathbf{U}(\tilde{\boldsymbol{\varepsilon}})J^{-1}\tilde{\phi}(\tilde{\boldsymbol{\varepsilon}}){:}\boldsymbol{\Phi}(\tilde{\boldsymbol{\varepsilon}})\mathbf{U}(\tilde{\boldsymbol{\varepsilon}}) = \tilde{\boldsymbol{\psi}}(\tilde{\boldsymbol{\varepsilon}}) \qquad (22)$$

where $\tilde{\boldsymbol{\phi}}$ and $\tilde{\boldsymbol{\psi}}$ are tensorial functions; $\tilde{\mathbf{S}} = \tilde{\boldsymbol{\phi}}(\tilde{\boldsymbol{\varepsilon}})$ defines the constitutive law in conjugate quantities; and $\mathbf{s} = \tilde{\boldsymbol{\psi}}(\tilde{\boldsymbol{\varepsilon}})$ defines the constitutive law in nonconjugate quantities. Function $\tilde{\boldsymbol{\psi}}(\tilde{\boldsymbol{\varepsilon}})$ is independent of rotation, which is requisite for a function defining the constitutive law [actual calculation of the function $\boldsymbol{\Phi}(\tilde{\boldsymbol{\varepsilon}})$ is difficult in the case of Hencky's tensor (Bažant 1998)].

Conjugacy of Micro-Macro Constraints

The algorithm for calculating the stress tensor from the strain tensor proceeds in the explicit microplane model in three steps: (1) Calculation of the microplane strain components ε_N, ε_M, and ε_L from Green's Lagrangian strain tensor ε_{ij} based on the kinematic constraint; (2) calculation of the nonconjugate microplane stresses $\hat{\sigma}_N$, $\hat{\sigma}_M$, and $\hat{\sigma}_L$ from ε_N, ε_M, and ε_L based on the microplane constitutive law; and (3) calculation of the back-rotated Cauchy stress tensor σ_{ij} from $\hat{\sigma}_N$, $\hat{\sigma}_M$, and $\hat{\sigma}_L$ based on the principle of virtual work.

The virtual work equation implied in the third step involves the strain tensor $\mathbf{e}$ and the microplane strains conjugate to the Cauchy stress tensor, and it implies a kinematic constraint between them (that is, the microplane strain components are the projections of the strain tensor onto the microplane). Thus it may seem that steps (1) and (3) are based on different kinematic constraints. By analogy with finite elements, in which the displacement interpolation functions used to calculate the strains in the element must be the same as those implied by the virtual work in calculating the nodal forces from the stresses, one might think there is a problem and suspect that this problem could cause negative energy dissipation, just as it would in such finite elements.

A similar problem, however, does not arise in the microplane model because there can be only one micro-macro kinematic constraint. If the Green's Lagrangian microplane strain components can be obtained by projecting Green's Lagrangian strain tensor, then, by definition, the microplane strain component conjugate to the back-rotated Cauchy stress tensor can be obtained by projecting the tensor $\mathbf{e}$. If the kinematic micro-macro constraint is imposed for one type of strain measure, then the kinematic constraint automatically holds for any other type of strain measure.

To further clarify why a similar problem does not arise, assume that we want to convert microplane strains ε_N, ε_M, and ε_L into the microplane strains e_N, e_M, and e_L corresponding to strain tensor $\mathbf{e} = [e_{ij}]$. There is no way to convert the strain components on one microplane alone into the components of another type of strain tensor (e.g., $\mathbf{e}$) on this microplane. We must first also know ε_N, ε_M, and ε_L for another (nonparallel) microplane, and only then do we have enough equations to invert the tensor projection giving the corresponding Green's Lagrangian strain tensor $\boldsymbol{\varepsilon}$. We can then convert this tensor into any other strain tensor, for example, $\mathbf{e}$. The only way to obtain the components of that other tensor for the microplane is to project it onto the microplane, that is, apply the kinematic constraint for that other tensor.

Therefore, it is irrelevant whether or not the micro-macro virtual work relation (step 3) implies the same conjugate strain tensor as the strain tensor that is actually used (step 1).

No Dissipation by Elastic Part of Strain

If the elastic strains could be large, as in rubber, a nonconjugate elastic stress-strain relation would be inadmissible, for it could lead to negative energy dissipation. However, in concrete as well as most structural materials and geomaterials, the elastic part of strains is always small. This means that the elastic part of the finite strain tensor could be replaced by the linearized (small) strain tensor, for which the elastic stresses and strains are automatically conjugate and thus cannot dissipate any energy (except for negligible errors of higher order). So the smallness of the elastic parts of strains saves the nonconjugate constitutive law from banishment.

Nonnegative Energy Dissipation by Inelastic Strains

In the explicit algorithm of the microplane model, the loading step in the inelastic range consists of two substeps: (1) An elastic increment $d\sigma^{el}$ going beyond the stress-strain boundary, followed by (2) an inelastic stress drop $d\sigma''$ representing a return to the boundary (Fig. 1) at constant strain. In other words, $d\sigma = d\sigma^{el} - d\sigma''$. This return is made at constant strain. Although our chosen strain measure is Green's Lagrangian, all the other strain measures are constant during the return, too, as already pointed out. Therefore, the strain tensor conjugate to the back-rotated Cauchy stress is constant during the inelastic stress drop (return to the stress-strain boundary), and so $d\sigma''$ represents a stress drop happening also at constant conjugate strain. The sign of $d\sigma''$ is always the same as the sign of σ, and so the total energy dissipation for one microplane is

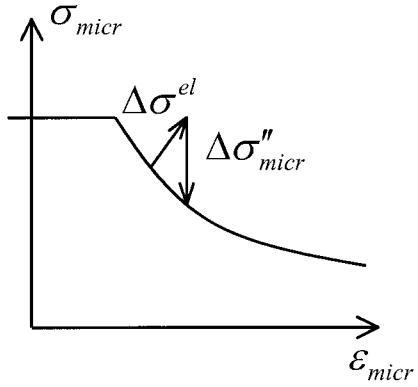

FIG. 1. Elastic Stress Increment beyond Boundary Followed by Inelastic Stress Drop to Boundary

$$d\bar{W}_d = \int (\sigma_N d\varepsilon''_N + \sigma_M d\varepsilon''_M + \sigma_L d\varepsilon''_L) = \int \left(\sigma_N \frac{d\sigma''_N}{C_N} + \sigma_M \frac{d\sigma''_M}{C_T} + \sigma_L \frac{d\sigma''_L}{C_T} \right) \geq 0 \tag{23}$$

where C_N and C_T are the elastic constants on the microplane level.

CONVENIENT STRAIN MEASURES AND MEMORY OF INITIAL STATE

For data fitting, it is convenient if the normal strain has a range of $(-\infty, \infty)$ and if the compression is symmetric to tension in the sense that the strain for stretch $1/\lambda$ equals minus the strain for stretch λ. Green's Lagrangian strain, however, has the range $(-0.5, \infty)$, and it does not possess the compression-tension symmetry. For the normal microplane strain, both these properties can be attained by redefining it as

$$\gamma_N = \frac{1}{2} \ln(1 + 2\varepsilon_N) \tag{24}$$

Likewise, the shear angle θ_{NM} or θ_{NL}, with its range $(-\pi/2, \pi/2)$, is not too convenient for setting up the microplane stress-strain relations. Instead of (19), it is preferable to define the microplane shear strain as

$$\gamma_{NL} = \frac{1}{2} \tan \theta_{NL} = \left(\frac{(1 + 2\varepsilon_N)(1 + 2\varepsilon_L)}{\varepsilon_L^2} - 4 \right)^{-1/2} \tag{25}$$

with a similar expression for γ_{NM}. This gives the shear strain measure the range $(-\infty, \infty)$.

In finite-strain generalization of model M4, however, the nonlinear parts of shear strains play no role because the frictional boundary of model M4 is independent of the shear strains or shear angles, and the elastic shear strains in concrete are always small. Therefore, the finite shear strains or finite shear angles (19) and (25) need not be calculated in model M4.

The expressions for the boundary curves in the microplane stress-strain space are total stress-strain relations that preserve memory of the initial (virgin) state of material. This memory constitutes a significant difference from the incremental plastic formulations for large deformations of metals, which have been handled by the incremental rate-based or updated Lagrangian formulations (McMeeking and Rice 1975; Bathe 1982; Bell 1985; Lubliner 1986; Gabriel and Bathe 1995; Hibbitt et al. 1995).

Despite memory, however, the present material model is not hyperelastic, for two reasons—first, for unloading, the microplane response is different (elastic, with the initial or degraded stiffness); and second, even for the case of monotonic loading on the macroscale, unloading may (and usually does) arise on some of the microplanes. There exists a vast number of different combinations of loading and unloading on different microplanes. Thus, the macroscopic response is generally path-dependent. The memory of the initial state exists only on each individual microplane, but not on the macroscale, that is, not on the continuum level of response.

FINITE-ELEMENT SIMULATIONS OF STRUCTURAL RESPONSE

To close the present series of four papers in this issue on the microplane model, it is now appropriate to present some examples of structural analysis. Model M4, generalized for rate effects and finite strain (Bažant et al. 2000b; Caner and Bažant 2000), has provided excellent results in finite-element simulations of experiments of two kinds: (1) The penetration of projectiles into concrete walls, with or without perforation of the wall; and (2) explosive ground shock. In the latter, large strains requiring finite-strain modeling were not reached, and the calculated deflections were almost exact. In the former, which require finite-strain simulation, the improved model predicted the deformations and fracturing of the perforated reinforced concrete wall quite accurately, yet the exit velocity of the missile was too high. The main reason for this discrepancy was that the model used in these simulations did not include the energy-dissipating rate effects modeled in the companion paper by Bažant et al. (2000a). The simulations, which were conducted at the Department of Defense Major Shared Resource Center at the Waterways Experiment Station (WES), utilize the explicit finite-element code (hydrocode) EPIC (Johnson et al. 1995), in which the finite-strain version of model M4 has been implemented.

In the first kind of experiments, Johnson and Cook's (1983) material strength models were used for the steel case and the filler. Slide lines were introduced between the explosive filler and the steel case of the projectile, and also between the projectile and the concrete target.

In one experiment of the first kind, reported by Forrestal et al. (1994), a projectile consisting of a hollow steel case and an inert explosive filler impacted orthogonally a concrete block large enough to be regarded as a halfspace, and penetrated deep into the block. The experiment was simulated with a 2D axisymmetric finite-element model, which included approximately 3,400 nodes and 6,700 continuum elements. Each

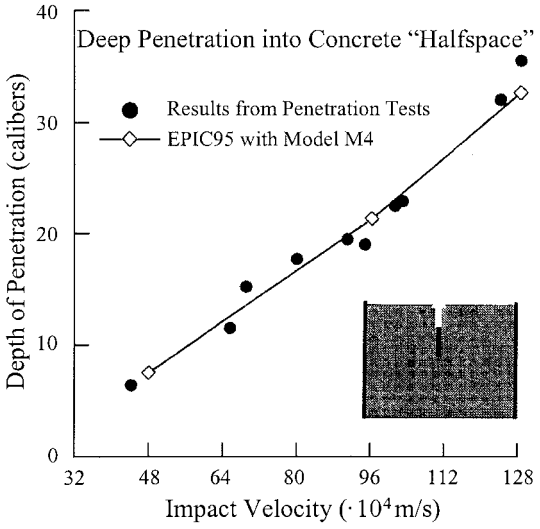

FIG. 2. Measured and Calculated Depth of Penetration into Halfspace of Normal Strength Concrete, Normalized by Projectile Diameter, versus Impact Velocity (m/s)

2D axisymmetric EPIC simulation required approximately 11.7 hours of CPU time on the Cray C90.

The simulation results are shown in Fig. 2, where the depth of penetration, normalized by the projectile diameter (i.e., the caliber), is plotted as a function of the impact velocity. The numerical simulations, made for three different impact velocities, agree with the experiments well. Because a significant portion of a deep penetration event occurs in the so-called ''tunneling'' mode, such good agreement could not have been achieved if the microplane model did not closely replicate the high-pressure ductile response of concrete.

In another experiment of the first kind, a thin concrete slab was perforated by a hollow steel projectile, impacting orthogonally to the slab. A 2D axisymmetric finite-strain finite-element model that comprised approximately 1,300 nodes and 2,500 continuum elements was used. To minimize the number of elements, their size was increased with the distance from the centerline of the impacting projectile. The so-called ''soaker'' elements (infinite elements) were used along the sides of the target so as to simulate energy radiations and thus avoid modeling the entire width of the target. Each simulation with EPIC required approximately 3.9 hours of CPU time on the Cray C90.

To demonstrate some of the results achieved, Fig. 3 shows the deformation of the target wall at the exit of the missile. The evidence of the formation of impact and exit craters, as represented by contours of the effective plastic strain ($\sqrt{J_2}$ of the inelastic part of the strain tensor), is particularly noteworthy (the classical concrete constitutive models based on plasticity, even with strain softening, have been proven incapable of simulating these craters). The final damage of the target wall predicted with the finite-strain microplane model is consistent with that observed after the experiments. These favorable results are attributed to the capability of the microplane model to simulate the low-pressure brittle behavior of concrete (Cargile et al. 1993; Adley et al. 1996). Due to the effect of free surfaces in this type of experiment, the target behaves predominantly as a brittle softening material, much like concrete in an unconfined uniaxial compression test.

The present computations were carried out before completing the generalization of the microplane model M4 for the material rate effects of fracturing and creep, presented in the companion paper by Bažant et al. (2000a). The dissipation associated with the loading rate was simply modeled in the EPIC program by artificial viscous damping dependent on the nodal velocities. Such an approach, however, cannot properly distinguish between the extremely high strain rates at the concrete-projectile interface and the much lower strain rates at points remote from the interface, nor capture the differences in the strain rate effects between compression and tension or among different triaxial loading paths. Introducing these effects into the finite-strain microplane model is expected to improve its predictive capability.

Since the microplane model exhibits strain softening, some form of a nonlocal or crack-band model would in principle be appropriate. However, the problems of spurious mesh sensitivity caused by strain softening [Bažant (1976); see also Bažant and Cedolin (1991), and Bažant and Planas (1998), discussed in Part I of this study] have been found practically negligible thanks to the extremely short duration of the impact or explosion events, the presence of viscosity effects (damping), and the very large inertia forces that dominate the response and delay localization beyond the duration of the event.

In an experiment of the second kind, a reduced-scale buried reinforced concrete structure was subjected to a ground shock caused by the detonation of a 1.84 kg sphere of C-4 explosive in the sand backfill above the roof (Fig. 4) (Akers et al. 1997; Philips et al. 1999). The objective of the 3D finite-strain simulation with the concrete microplane model was to predict the dynamic interaction of the structure with the soil medium, and especially the response of the roof slab. The mesh used in the numerical simulation (Fig. 4) included five zones: (1) The finely meshed concrete structure; (2) the finely meshed layer of soil backfill surrounding the structure; (3) the coarser meshed soil backfill behind the layer; (4) the chanber wall of the blast load generator; and (5) a cavity of radius 25 cm in the soil backfill. The reinforcing steel in the structure was modeled with bar elements using the Johnson-Cook material strength model. The fracture of these elements was simulated using Johnson and Cook's (1985) fracture model. The soil backfill was simulated using the hybrid elastic-plastic (HEP) model for sand implemented in EPIC at WES. The time history of the radial stress components at the points on the inner surface of the spherical cavity was prescribed. The values to

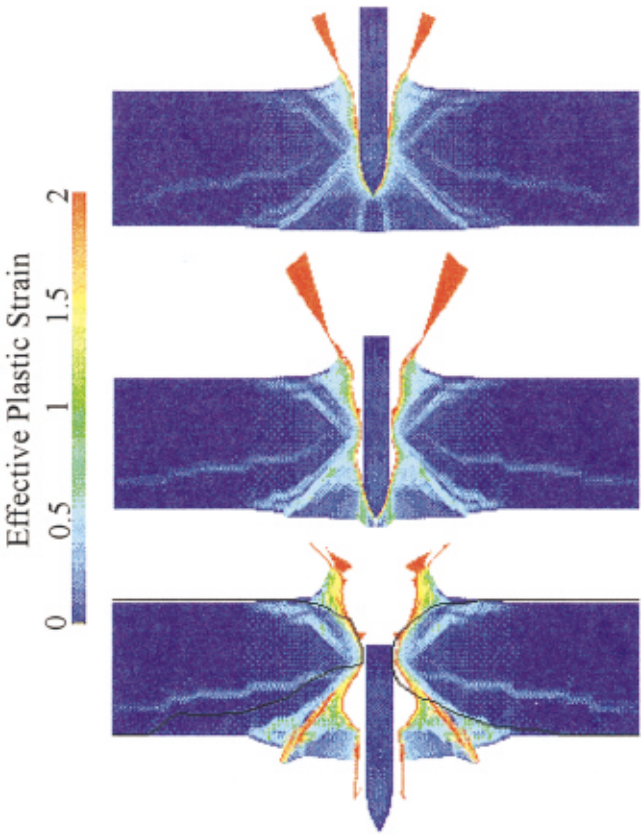

FIG. 3. Simulation with Finite-Element Code EPIC of Perforation of Concrete Wall

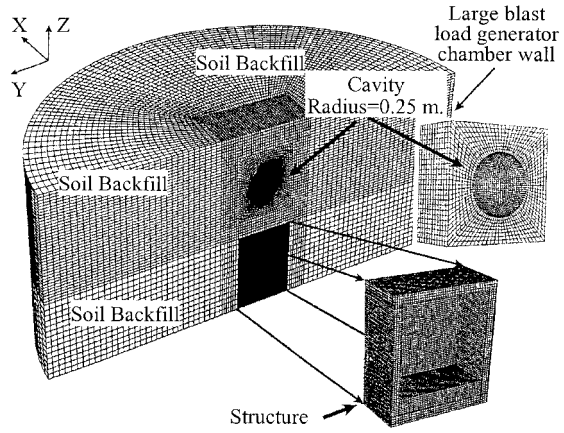

FIG. 4. Finite-Element Mesh for Reinforced Concrete Structure Buried in Soil

be prescribed were determined in advance by conducting a 1D spherical shock calculation within the range of 0.25 m.

A 3D mesh involving 250,000 nodes, 230,000 brick elements, and 23,000 bar elements was used in these simulations (Fig. 4). Approximately 40,000 of the brick elements involved the finite-strain generalization of the microplane model. The calculation of the maximum deflections of the roof slab (Fig. 5) required approximately 160 CPU hours on the Cray C90.

The HEP soil model (Zimmerman et al. 1987; Akers and Adley 1995; Akers et al. 1995) was specifically designed for calculating ground shock from conventional weapons. The model accurately replicates the complex shear-strain behavior of ductile geologic materials and can be fit to typical WES laboratory test data. The laboratory calibrations of the model have been validated by a number of scaled explosive field tests. The HEP model uses constant Poisson ratio values for loading and unloading and involves a complex pressure-volume algorithm that employs an exponential pressure-dependent shear failure surface with a complex pressure-volume algorithm. This surface, which relates the pressure and the second invariant of the stress deviator, was fit to quasistatic laboratory data for triaxial compression failure. The HEP model also features a modified Tillotson equation of state (EOS) to calculate the energy-dependent pressure-volume response of materials. The EOS decomposes the pressure into two components: the first represents the energy-independent total hydrostatic response of the solids, air, and pore water in the soil, while the second represents an energy-dependent pressure term. An energy-independent hysteretic EOS is used to calculate the dependence of the volume compression on the pressure for both loading and unloading in the positive (compressive) and negative (tensile) pressure ranges. This energy-independent EOS is nonhysteretic after the voids close, the state of void closure being determined by the fitting process.

Comparisons with measurements showed that the calculated stresses and velocities in the soil backfill were identical at output stations located beyond the influence of the structure and at various equivalent ranges from the explosive charge. The calculated interface stresses at the center of the roof slab of the structure indicated that, up to the time of 2 ms, the loading was dominated by shock wave propagation and controlled by the relative impedances and wave speeds in the sand, concrete, and air. A very good agreement was obtained between the calculated peak particle velocities and the corresponding free-field ground shock data. The roof slab suffered only moderate damage during the experiment. The final deflection profiles of the roof slab measured after the experiment across two perpendicular vertical cross sections of the structure are compared with the calculated profile in Fig. 5. The agreement with the predictions based on the microplane model is excellent.

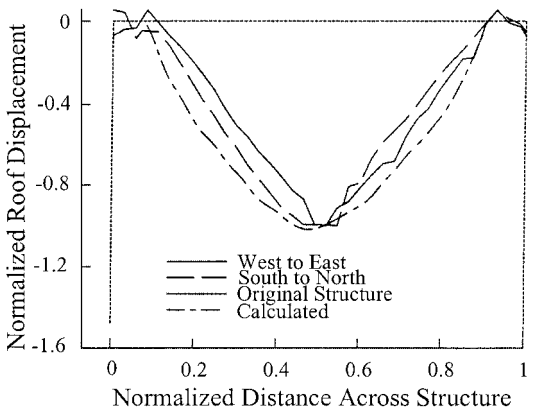

FIG. 5. Measured and Calculated Profile of Maximum Deflection of Roof Slab Obtained with Finite-Element Mesh in Fig. 4

Although EPIC is highly optimized for the CRAY vector machines, the microplane model has not yet been optimized for any specific computing platform. Therefore the aforementioned CPU time of 160 hours on the Cray C90 doubtless greatly exceeds the achievable time. Most of the CPU time used in explicit dynamic finite-element simulations is generally required for elemental computations, unless there are numerous complex sliding interfaces.

Consequently, optimization of the subroutines used to implement the microplane model and its finite-strain generalization would likely reduce the overall CPU time significantly. It is expected that the basic optimization of these subroutines for the CRAY C90 vector machine could easily reduce the CPU time required by the microplane model by a factor of two to four, and aggressive optimization for either vector or parallel computing platforms could lead to an even better performance. Furthermore, since the present microplane computation used Stroud's (1971) 28-point optimal Gaussian formula for integration over a unit hemisphere, a further reduction could be achieved by replacing it with Bažant and Oh's (1986) 21-point formula, which has just been found nearly as accurate.

The results make it already clear that the availability of high-power large computers and workstations has made the microplane constitutive model viable even for complex 3D problems.

CONCLUSIONS

1. For the formulation of the microplane model as well as other sophisticated finite-strain constitutive relations for frictional (pressure-sensitive) materials such as concretes, soils, rocks and some composites, it is convenient to use a stress tensor referred to the initial configuration that has a clear physical meaning, such that the stress components on any plane give in a simple way the true (Cauchy) normal and shear stresses on that plane, and that the hydrostatic pressure is easily controlled. Only then is it easy to model friction, yield or strength limit, and hardening or softening on that plane. The stress tensor referred to the initial configuration that satisfies these conditions is the back-rotated Cauchy stress tensor, which has been adopted in this study. Another, only slightly less convenient, would be the back-rotated Kirchhoff stress tensor.
2. The strain tensors conjugate to the back-rotated Cauchy and Kirchhoff stress tensors are nonholonomic, that is, their values depend on the strain path. This property makes them unsuitable for quasibrittle materials such as concrete that have a memory of their initial state.
3. For the sake of simplicity and clarity, it is desirable that the strain tensor components on one microplane suffice to fully characterize the stretch (relative change of length) of a material line segment initially normal to that microplane and the true shear angle on that microplane (change of the angle between the initial normal and the microplane). This condition is satisfied only by Green's Lagrangian finite-strain tensor. For any other strain tensor, the aforementioned stretch and shear angle on one microplane depend also on the strain tensor components or planes of other orientation, which would greatly complicate the formulation of a microplane constitutive model.
4. Consequently, it is best to base the finite-strain microplane model on Green's Lagrangian strain tensor and the back-rotated Cauchy stress tensor, even though they are not conjugated by work. Transformation of the constitutive relation to conjugate strain and stress tensors (e.g., Green's Lagrangian strain tensor and the second Piola-

Kirchhoff stress tensor) is of course generally possible, but the resulting complexity would defeat the purpose of microplane approach—the conceptual simplicity and intuitive clarity.

5. The adoption of nonconjugate strain and stress tensors for a microplane model of concrete is admissible because the following four conditions are satisfied: (1) The adopted nonconjugate constitutive law on the microplane level is in unique correspondence to a certain conjugate constitutive law on the macrolevel. (2) The micro-macro kinematic constraint of the microplane model imposed in terms of one type of strain tensor implies that the kinematic constraint holds also for any other finite-strain tensor. (3) The elastic parts of strains are always small, which ensures the energy dissipation caused by elastic deformations formulated in terms of the nonconjugate stress and strain tensors to be negligible. (4) The drops of inelastic stress to the boundary surface, which are made in the numerical algorithm at constant strain, always dissipate energy (i.e., a negative energy dissipation is ruled out).
6. Because the volume changes of concrete can never be large, the split of strains and stresses into their volumetric and deviatoric components can be considered as additive if the volumetric and deviatoric strain definitions from Bažant (1996) are employed. This greatly simplifies the finite-strain generalization of the microplane model.
7. Extended to the rate effect and finite strain, model M4 gives realistic predictions in vectorized explicit finite-element simulations of missile impact and ground shock on concrete structures.

APPENDIX I. STRAIN TENSORS CONJUGATE TO ROTATED CAUCHY AND KIRCHHOFF STRESS TENSORS

The strain tensor $\mathbf{e}$ conjugate to the back-rotated Cauchy stress tensor $\mathbf{s}$ (8) may be defined by the following variational equation stating the equivalence of the virtual work per unit initial volume of the material: $\delta\mathbf{e}:\boldsymbol{\sigma} = \delta\boldsymbol{\varepsilon}:\mathbf{S}$, where $\boldsymbol{\varepsilon}$ = Green's Lagrangian strain tensor and $\mathbf{S}$ = second Piola-Kirchhoff stress tensor. Substituting (8) and (2) for $\boldsymbol{\sigma}$ and $\mathbf{S}$, we have $\delta\mathbf{e}:\mathbf{R}^T J\boldsymbol{\sigma}\mathbf{R} = \delta\boldsymbol{\varepsilon}:\mathbf{F}^{-1}\boldsymbol{\sigma}\mathbf{F}^{-T}$. Introducing the polar decomposition of the deformation gradient, $\mathbf{F} = \mathbf{R}\mathbf{U}$, denoting $\mathbf{Y} = \mathbf{U}^{-1}$ and $\mathbf{Z} = \mathbf{R}^T\boldsymbol{\sigma}\mathbf{R}$ (and noting that $\mathbf{F}^{-1} = \mathbf{U}^{-1}\mathbf{R}^T$, $\mathbf{F}^{-T} = \mathbf{R}\mathbf{U}^{-1}$), we get $\delta\mathbf{e}:\mathbf{Z} = \delta\boldsymbol{\varepsilon}:\mathbf{Y}\mathbf{Z}\mathbf{Y}J$ or $\delta\mathbf{e}_{ij}Z_{ij} = \delta\varepsilon_{kl}Y_{ki}Y_{jl}Z_{ij}J$. This equation must be satisfied for any Z_{ij}. This is possible if and only if $\delta\mathbf{e}_{ij} = Y_{jl}\delta\varepsilon_{lk}Y_{ki}J$. Noting that $\boldsymbol{\varepsilon} = (\mathbf{U}^2 - \mathbf{I})/2$ and $\delta\boldsymbol{\varepsilon} = \delta(\mathbf{U}\mathbf{U})/2$, and changing variation δ to differential d, we thus conclude that the strain tensor $\mathbf{e}$ that is conjugate to the back-rotated Cauchy stress is defined incrementally as follows (Bažant 1997):

$$d\mathbf{e} = \mathbf{U}^{-1}d\boldsymbol{\varepsilon}\mathbf{U}^{-1}J = \frac{J}{2}\,\mathbf{U}^{-1}(d\mathbf{U}\mathbf{U} + \mathbf{U}d\mathbf{U})\mathbf{U}^{-1} \qquad (26a)$$

$$d\mathbf{e} = \frac{J}{2}\,(\mathbf{U}^{-1}d\mathbf{U} + d\mathbf{U}\mathbf{U}^{-1}) = J\,\mathrm{sym}(\mathbf{U}^{-1}d\mathbf{U}) \qquad (26b)$$

The strain increment $d\mathbf{e}$ can also be expressed in terms of the current deformation rate tensor $\mathbf{D}$, which has the components $D_{ij} = (v_{i,j} + v_{j,i})/2 = \mathrm{sym}(v_{i,j})$, where $v_i = \dot{x}_i$ = velocity vector of material point. To relate $\mathbf{D}$ to $\mathbf{F}$, we note that the rate of work of Cauchy stress per current volume J must be equal to the rate the second Piola-Kirchhoff stress $\mathbf{S}$ per unit initial volume, that is, $J\boldsymbol{\sigma}:\mathbf{D} = \mathbf{S}:\dot{\boldsymbol{\varepsilon}}$. The superior dot denotes the time rate. Substituting $\mathbf{S} = \mathbf{F}^{-1}J\boldsymbol{\sigma}\mathbf{F}^{-T}$, we get the variational equation $\boldsymbol{\sigma}:\mathbf{D} = \mathbf{F}^{-1}\boldsymbol{\sigma}\mathbf{F}^{-T}:\dot{\boldsymbol{\varepsilon}}$ or, in coordinate notation, $S_{jk}D_{jk} = Q_{ij}S_{jk}Q_{lk}\dot{\varepsilon}_{il}$ or $S_{jk}(D_{jk} - Q_{ij}\dot{\varepsilon}_{il}Q_{lk}) = 0$, where $\mathbf{Q} = \mathbf{F}^{-1}$, with components Q_{ij}. This equation must be satisfied for any S_{jk}. This is possible if and only if the expression in the parentheses vanishes, that is, $D_{jk} = Q_{ij}\dot{\varepsilon}_{il}Q_{lk}$ or $\mathbf{D} = \mathbf{F}^{-T}\dot{\boldsymbol{\varepsilon}}\mathbf{F}^{-1}$. It follows that $d\mathbf{e} = \mathbf{R}^T\mathbf{D}\mathbf{R}Jdt$, where t = time. For no rotation, $d\mathbf{e} = \mathbf{D}Jdt$.

Consider now the special case of deformation history during which the principal axes of $\mathbf{U}$ do not rotate against the material, as is typical of most types of laboratory tests. We may now place the coordinate axes x_i in the principal directions. Then $\mathbf{U}$ is diagonal, with the diagonal components representing the principal stretches λ_I (I = 1, 2, 3). Eq. (26) yields $d\mathbf{e}_1 = Jd\varepsilon_2/\lambda_1^2 = \lambda_2\lambda_3 d\lambda_1$, and permutated expressions for $d\mathbf{e}_2$ and $d\mathbf{e}_3$, which provides the matrix expression (10). The result in (10), of course, could have been obtained directly from the virtual work relation in principal coordinates, $\Sigma_I\ \sigma_I\delta\xi_I = \Sigma_I\ S_I\delta\varepsilon_I$. For nonrotating principal axes, $S_I = \sigma_I/\lambda_1^2$ and $\delta\varepsilon_I = \lambda_I\delta\lambda_I$. In a similar manner, starting from the virtual work relation $\delta\boldsymbol{\xi}:\boldsymbol{\tau} = \delta\boldsymbol{\varepsilon}:\mathbf{S}$, one can show that $d\boldsymbol{\xi} = \mathbf{R}^T\mathbf{D}\mathbf{R}dt$. For nonrotating principal strain axes, $d\xi = \mathbf{D}dt$, which yields the matrix expression (9).

To check how pronounced the path dependence of $\boldsymbol{\xi}$ may be, consider two loading paths leading to the same final state $\lambda_{11} = 1 + e$, $\lambda_{12} = e$, with all the other components of the stretch tensor remaining constant. Path I represents proportional (radial) loading. For path II, λ_{11} is first increased to the value $1 + e$ while all the other stretch tensor components remain constant, and then λ_{12} is increased to the value e while no other stretch tensor component increases. For these two paths, it is easy to integrate (26) exactly, by closed-form expressions. The maximum principal values ξ^I and ξ^{II} of $\boldsymbol{\xi}$ for the coinciding final states of paths I and II have been calculated (Bažant 1997). For e = 0.001, 0.01, 0.1, 0.25, 0.5, 1, 2, and 4, the percentage deviations of ξ^{II} from ξ^I have been obtained as −0.028, −0.276, −2.67, −6.40, −12.37, −25.9, −86.0, and −89.1%, respectively. These results show that, for maximum stretches up to about 10%, the deviation of $\boldsymbol{\xi}$ from the Hencky (logarithmic) strain is negligible, but not for larger stretches. The path-dependence of $\mathbf{e}$ is about equally strong.

DEDICATION

Dedicated to Prof. Dietmar Gross, Darmstadt, on the occasion of his 60th birthday.

ACKNOWLEDGMENTS

Partial financial support under contract DACA-96K-0049 between the Waterways Experiment Station (WES), Vicksburg, Mississippi, and Northwestern University (monitored by Dr. J. Zelasko) is gratefully acknowledged. Additional partial funding for the nondynamic aspects of the model was obtained under NSF Grant CMS-9713944 to Northwestern University.

APPENDIX II. REFERENCES

Adley, M. D., Cargile, J. D., Akers, S. A., and Rohani, B. (1996). "Numerical simulation of projectile penetration into concrete." *Proc., 14th U.S. Army Symp. on Solid Mech.*, Myrtle Beach, S.C.

Akers, S. A., and Adley, M. D. (1995). "Constitutive models for geologic materials implemented into the EPIC code." *Proc., 66th Shock and Vibration Symp.*, Biloxi, Miss.

Akers, S. A., Adley, M. D., and Cargile, J. D. (1995). "Comparison of constitutive models for geologic materials used in penetration and ground shock calculations." *Proc., 7th Int. Symp. on Interaction of Conventional Munitions with Protective Struct.*, Mannheim, Germany.

Akers, S. A., Phillips, B. R., Windham, J. E., and Rickman, D. D. (1997). "Numerical simulations of the small-scale structure-medium-interaction 2 experiment." *Proc., 68th Shock and Vibration Symposium*, Hunt Valley, Md.

Bažant, Z. P. (1976). "Instability, ductility, and size effect in strain-softening concrete." *J. Engrg. Mech.*, ASCE, 102(2), 331–344.

Bažant, Z. P. (1996). "Finite strain generalization of small-strain constitutive relations for any finite strain tensor and additive volumetric-deviatoric split." *Int. J. Solids and Struct.*, 33(20–22), 2887–2897 (special issue in memory of Juan Simo).

Bažant, Z. P. (1997). ''Recent advances in brittle-plastic compression failure: Damage localization, scaling and finite strain.'' *Computational plasticity: Fundamentals and applications, Proc., 5th Int. Conf. on Comp. Plasticity*, D. R. J. Owen, E. Oñate, and E. Hinton, eds., International Center for Numerical Methods in Engineering, Barcelona, Spain, 3–19.
Bažant, Z. P. (1998). ''Easy-to-compute tensors with symmetric inverse approximating Hencky finite strain and its rate.'' *J. Engrg. Mat. and Technol.*, 120(2), 131–136.
Bažant, Z. P., Bishop, F. C., and Chang, T.-P. (1986). ''Confined compression tests of cement paste and concrete up to 300 ksi.'' *J. Am. Concrete Inst.*, 83, 553–560.
Bažant, Z. P., and Oh, B.-H. (1986). ''Efficient numerical integration on the surface of a sphere.'' *Zeitschrift für angewandte Mathematik und Mechanik*, Berlin, 66(1), 37–49.
Bažant, Z. P., and Cedolin, L. (1991). *Stability of structures: Elastic, inelastic, fracture and damage theories*, Oxford University Press, New York, Sec. 11.1–11.4.
Bažant, Z. P., Xiang, Y., and Prat, P. C. (1996). ''Microplane model for concrete. I: Stress-strain boundaries and finite strain.'' *J. Engrg. Mech.*, ASCE, 122(3), 245–254; with errata, Vol. 123 (1997).
Bažant, Z. P., and Planas, J. (1998). *Fracture and size effect in concrete and other quasibrittle materials*, CRC Press, Boca Raton, Fla., and London.
Bažant, Z. P., Kim, J.-H., and Brocca, M. (1999). ''Finite strain tube-squash test for concrete at high pressure and shear angles up to 70°.'' *Struct. Engrg. Rep. 98-5/C407f*, Northwestern University; *ACI Mat. J.*, 96(5), 580–592.
Bažant, Z. P., Caner, F. C., Adley, M. D., and Akers, S. A. (2000a). ''Fracturing rate effect and creep in microplane model for dynamics.'' *J. Engrg. Mech.*, ASCE, 126(9), 962–970.
Bažant, Z. P., Caner, F. C., Carol, I., Adley, M. D., and Akers, S. A. (2000b). ''Microplane model M4 for concrete: I: Formulation with work-conjugate deviatoric stress.'' *J. Engrg. Mech.*, ASCE, 126(9), 944–953.
Bathe, K. J. (1982). *Finite element procedures in engineering analysis*, Prentice-Hall, Englewood Cliffs, N.J.
Bell, J. F. (1985). ''Contemporary perspectives in finite strain plasticity.'' *Int. J. Plasticity*, 1, 3–27.
Biot, M. A. (1965). *Mechanics of incremental deformations*, Wiley, New York.
Caner, F. C., and Bažant, Z. P. (2000). ''Microplane model M4 for concrete. II: Algorithm, calibration and application.'' *J. Engrg. Mech.*, ASCE, 126(9), 954–961.
Cargile, J. D., Giltrud, M. E., and Luk, V. K. (1993). ''Perforation of thin unreinforced concrete slabs.'' *6th Int. Symp. on Interaction of Non-Nuclear Munitions with Structures*, Panama City Beach, Fla.
Carol, I., Jirásek, M., Bažant, Z. P., and Steinmann, P. (1998). ''New thermodynamic approach to microplane model with application to finite deformations.'' *Tech. Rep. PI-145*, International Center for Numerical Methods in Engineering (CIMNE), Barcelona, Spain.
Doyle, T. C., and Ericksen, J. L. (1956). ''Non-linear elasticity.'' *Advances in Applied Mechanics*, 4, 53–115.
Eterovic, A. L., and Bathe, K. J. (1990). ''A hyperelastic-based large-strain elastoplastic constitutive formulation.'' *Int. J. Numer. Methods in Engrg.*, 30, 1099–1114.
Flory, T. J. (1961). ''Thermodynamic relations for high elastic materials.'' *Trans., Faraday Soc.*, 57, 829–838.
Forrestal, M. J., Altman, B. S., Cargile, J. D., and Hanchak, S. J. (1994). ''An empirical equation for penetration depth of ogive-nose projectiles into concrete targets.'' *Int. J. Impact Engrg.*, 15(4), 395–405.
Gabriel, G., and Bathe, K. J. (1995). ''Some computational issues in large strain elasto-plastic analysis.'' *Comp. and Struct.*, 56(2/3), 249–267.
Hencky, H. (1928). ''Über die Form des Elastizitätsgesetzes bei ideal elastischen Stoffen.'' *J. Rheology*, 2, 169–176.
Hibbitt, H. D., Karlsson, B. I., and Sorensen, P. (1995). *ABAQUS theory manual (1994), Version 5.5*, Hibbitt, Karlsson & Sorensen, Inc., Pawtucket, R.I., Sec. 4.6.1.
Hoger, A. (1987). ''The stress conjugate to logarithmic strain.'' *Int. J. Solids and Struct.*, 23(12), 1645–1656.
Jirásek, M. (1999). ''Comments on microplane theory.'' Mechanics of quasi-brittle materials and structures: A volume in honor of Prof. Bažant's 60th birthday, G. Pijaudier-Cabot, Z. Bittnar, and B. Gérard, eds., Hermès Science Publications, Paris, 57–78.
Johnson, G. R., and Cook, W. H. (1983). ''A constitutive model and data for metals subjected to large strains, high strain rates, and high temperatures.'' *Proc., 7th Int. Symp. on Ballistics*, The Hague, The Netherlands.
Johnson, G. R., and Cook, W. H. (1985). ''Fracture characteristics of three metals subjected to various strains, strain rates, temperatures and pressures.'' *Engrg. Fracture Mech.*, 21.
Johnson, G. R., Stryk, R. A., and Holmquist, T. J. (1995). *User instructions for the 1995 version of the EPIC Research Code*, Alliant Techsystems, Hopkins, Minn.
Levitas, V. I. (1996). *Large deformation of materials with complex rheological properties at normal and high pressure*, Nova Science Publishers, New York.
Lubliner, J. (1986). ''Normality rules in large-deformation plasticity.'' *Mech. of Mat.*, 5, 29–34.
Malvern, L. E. (1969). *Introduction to the mechanics of a continuous medium*, Prentice-Hall, Englewood Cliffs, N.J.
McMeeking, R. M., and Rice, J. R. (1975). ''Finite-element formulations for problems of large elasto-plastic deformation.'' *Int. J. Solids and Struct.*, 11, 601–616.
Ogden, R. W. (1984). *Non-linear elastic deformations*, Ellis Horwood, Ltd., Chichester, U.K. and Wiley, Chichester, U.K.
Philips, B. R., Windham, J. E., Woodson, S. C., and Rickman, D. D. (1999). ''Results of small-scale structure-medium interaction experiments.'' *Tech. Rep.*, U.S. Army Engineer Waterways Experiment Station, Vicksburg, Miss., in preparation.
Rice, J. R. (1993). ''Mechanics of solids.'' *Encyclopaedia Britannica*, 15th ed., Vol. 23, 737–747 and 773.
Sidoroff, F. (1974). ''Un modèle viscoélastique non linéaire avec configuration intermédiaire.'' *J. Méchanique*, Paris, 13, 679–713.
Simo, J. C. (1988). ''A framework for finite strain elastoplasticity based on maximum plastic dissipation and the multiplicative decomposition.'' *Comp. Methods in Appl. Mech. Engrg.*, 66, 199–219, and 68, 1–31.
Simo, J. C., and Ortiz, M. (1985). ''A unified approach to finite deformation elastoplastic analysis based on the use of hyperelastic constitutive equations.'' *Comp. Methods in Appl. Mech. and Engrg.*, 49, 221–245.
Stroud, A. H. (1971). *Approximate calculation of multiple integrals*, Prentice-Hall, Englewood Cliffs, N.J.
Zimmerman, H. D., Wagner, M. H., Carney, J. A., and Ito, Y. M. (1987). ''Effects of site geology on ground shock environments. Report 1: Constitutive models for materials I2, I3, and W1-W10.'' *Tech. Rep. SL-87-19*, U.S. Army Engineer Waterways Experiment Station, Vicksburg, Miss.